

Preparation and characterization of mesoporous carbons using a Turkish natural zeolitic template/furfuryl alcohol system

Billur Sakintuna¹, Yuda Yürüm*

Faculty of Engineering and Natural Sciences, Sabanci University, Orhanli, Tuzla, Istanbul 34956, Turkey

Received 25 January 2006; received in revised form 3 March 2006; accepted 7 March 2006

Available online 24 April 2006

Abstract

The template carbonization method was utilized for the production of mesoporous carbons using a Turkish natural zeolite as a template. The major carbon precursor used was furfuryl alcohol. Furfuryl alcohol was polymerized and carbonized between 700 °C and 1000 °C in the channels of the natural zeolite. The structure of the zeolite template and carbons were investigated by surface analysis techniques, scanning electron microscopy, ¹³C NMR and FTIR spectrometry, and powder X-ray diffraction. At the micrometer level, the carbon material templated with the natural zeolite had the same morphology as the zeolite. The porous carbon samples contained 91–99% C and minor amounts of oxygen. While the surface area of the carbon produced without templation was only 18 m²/g, the surface area of the carbons produced within the template was found to be in the range of 400–800 m²/g. Average pore diameter of the porous carbons was measured as ca. 5–10 nm, demonstrating presence of mesoporous framework in the carbons. The ¹³C NMR and FTIR spectra revealed that the carbons produced in the carbonization range of 700–1000 °C contained some hydrogen and oxygen containing functional groups. The XRD results put forward indications to the presence of turbostratic structures and preservation of the structural regularity of the zeolite over extended distances in the carbons.

© 2006 Elsevier Inc. All rights reserved.

Keywords: Natural zeolite; Clinoptilolite; Templated carbons; Mesoporous carbon; Carbonization

1. Introduction

Porous carbon materials with high surface areas and large pore volumes have recently received much consideration because of their possible uses as adsorbents, catalysts, electrodes, and hydrogen storage systems [1,2]. Porous carbons are widely used as industrial adsorbents because of the hydrophobic nature of their surfaces, high surface area, large pore volumes, chemical inertness, good mechanical stability and good thermal stability. Application areas are wide, including gas separation, water purification, catalyst support, chromatography columns, storage of natural

gas, and use as electrodes of an electric double-layer capacitor [1,3–5]. The synthesis of new porous materials is interesting for both practical and fundamental reasons. The pore size distribution and topology of pores in materials of similar compositions can be very different, depending on the method of synthesis. The types of pores as defined by IUPAC are micropores, pores with width not exceeding about 2.0 nm (20 Å), mesopores, pores with width between 2.0 nm (20 Å) and 50 nm (500 Å) and macropores, pores with width exceeding about 50 nm (500 Å) [6].

Porous carbons are usually obtained via carbonization of precursors of natural or synthetic origin, followed by activation. To meet the requirements, a recent approach, the template carbonization method, has been proposed. Replication, the process of filling the pores of a solid with a different material, and chemically separating the resulting material from the template, is a technique that is widely

* Corresponding author. Tel.: +90 216 483 9512; fax: +90 216 483 9550.
E-mail address: yyurum@sabanciuniv.edu (Y. Yürüm).

¹ Present address: LIMHP-CNRS, Université Paris 13, 99 Avenue J.B. Clément, 93430 Villetaneuse, France.

used in microporosity and printing. This method has been used to prepare replica polymers [7,8], metals [9] and semi-conductors [10] and other materials [11,12].

Zeolites represent an interesting template for replication processes, because the dimensions of their cages and channels are quite similar to the size of organic molecules that constitute the replica. If such a nanospace in a zeolite is packed with carbon and then the carbon are liberated from the zeolite framework, one can expect the formation of a porous carbon whose structure reflects the porosity of the original zeolite template. Zeolites with three-dimensional pore structures were found to be suitable as templates [13,14], whereas zeolites with one-dimensional structures were not effective [15]. These carbons obtained using zeolite templates with three-dimensional pore structures retained the shapes of zeolite particles [16–20].

The template carbonization method has been utilized for the production of mesoporous carbons using a Turkish natural zeolite as a template, in the existing study. The main original aspect of the present work lies on the utilization of a native natural zeolite as a template. Natural zeolites have not been explored earlier as templates for the production of mesoporous carbon materials. In the present report, the effect of different templating mixtures and different carbonization temperatures on the structure of carbons were studied.

2. Experimental section

2.1. Template material

Turkish Manisa Gördes zeolite, obtained from Enli Mining Corp., Izmir, Turkey, was used as the porous template medium in the present work. Clinoptilolite was the predominant mineral (95%) present in the natural zeolite used. Average particle size was approximately 30 μm and BET surface area of the zeolite was 59.4 m^2/g . Chemical analyses of the zeolite are given in Table 1 and SEM image is presented in Fig. 1.

2.2. Synthesis procedure

2.2.1. Natural zeolite-templated porous carbons obtained from furfuryl alcohol (FA)

The synthesis of zeolite templated carbons followed approximately the techniques of the synthesis developed by Kyotani et al. [13]. FA was mixed with zeolite in a ratio of 10 ml FA/g zeolite, at room temperature for 5 days. The zeolite and FA mixture was then centrifuged at 2500 rpm for 30 min. The FA remained in pores of zeolite was polymerized under argon flow at 110 ml/min at 80 °C for 24 h, after which the temperature was raised to 150 °C for 8 h. The resulting polyfurfuryl alcohol (PFA)/zeolite composite was carbonized under 110 ml/min argon flow at 700, 800, 900 and 1000 °C and kept at the carbonization temperature for 3 h. To dissolve clinoptilolite template, the carbonized PFA/zeolite composite was washed with excess amount of

Table 1
Analyses of Turkish Manisa Gördes natural zeolite

% Clinoptilolite	95
Particle size	–30 μm
<i>Porous structure (vol.%)</i>	
Micropores	40.2
Mesopores	57.9
Macropores	1.9
<i>Chemical analysis (%)</i>	
SiO ₂	70.9
Al ₂ O ₃	12.4
K ₂ O	4.46
CaO	2.54
Fe ₂ O ₃	1.21
MgO	0.83
Na ₂ O	0.28
TiO ₂	0.09
P ₂ O ₅	0.02
MnO	<0.01

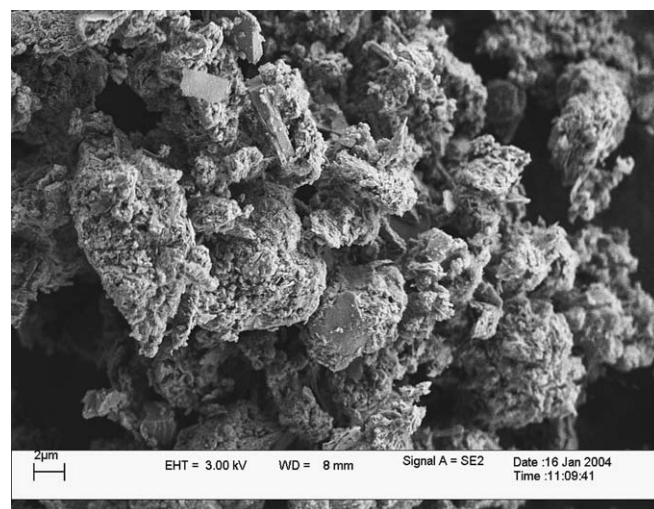


Fig. 1. SEM images of Turkish Manisa Gördes natural zeolite.

aqueous hydrofluoric acid (HF) solution (10%, by volume) at room temperature for 24 h. The resulting carbon was filtered and washed at least three times with water (200 ml each) to wash out the impurities and dried in an oven at 100 °C under a nitrogen atmosphere to prevent oxidation.

2.2.2. Carbon material produced without templation

A blank experiment to produce carbon material without templation was conducted: furfuryl alcohol (5 mg) was polymerized with oxalic acid (1 mg) as catalyst and the product was carbonized under 110 ml/min argon flow at 700 °C. All the carbonaceous material obtained throughout the study was kept under a nitrogen atmosphere to prevent oxidation and characterized by SEM, EDS and BET techniques.

2.2.3. Porous carbon obtained from sol–gel process using tetraethoxy silane (TEOS) in the presence of a natural zeolite and furfuryl alcohol (FA)

A silica sol was prepared by stirring a mixture of TEOS, ethyl alcohol, water and zeolite at 80 °C for 3 h. The mole

ratio of TEOS, ethyl alcohol, and water was 1:4:2. Zeolite was used as an acid source. Zeolite (6 g) was mixed with 60 ml TEOS/ethyl alcohol/water mixture. After the mixture was cooled in an ice bath, furfuryl alcohol, as a carbon precursor, was added to the silica sol (FA/silica sol = 2.00 vol/vol). This mixture was mixed at 120 °C for 2 h. Gelation and polymerization took place in this step. Then the polymerized FA/silica gel was carbonized at 700 °C under 110 ml/min argon flow and held at this temperature for 3 h to carbonize the polymerized FA. The carbonized composite was washed with excess amount of aqueous HF solution (10%, by volume) at room temperature to dissolve clinoptilolite template for 24 h. The resulting carbon (TEOS–PFA) was filtered and washed three times with water (200 ml each), and dried in an oven at 100 °C under a nitrogen atmosphere to prevent oxidation.

2.2.4. Natural zeolite-templated porous carbon obtained from FA and TEOS mixture

FA and TEOS mixture (FA/TEOS = 9 vol/vol) was mixed with zeolite in a ratio of 10 ml mixture/g zeolite, at room temperature for 5 days. The zeolite and FA/TEOS mixture was then centrifuged at 2500 rpm for 30 min. The FA impregnated in the zeolite together with TEOS was polymerized at 80 °C for 24 h under argon flow at 110 ml/min, after which the temperature was raised to 150 °C for 8 h. In order to carbonize, the polymerized FA/zeolite composite was heated to 700 °C at a 5 °C/min rate and kept there for 3 h. The carbonized FA/zeolite composite was washed with excess amount of aqueous HF solution (10%, by volume) at room temperature to dissolve clinoptilolite template for 24 h. The resulting carbon was filtered and washed at least three times with water (200 ml each) to wash out the impurities and dried in an oven at 100 °C under a nitrogen atmosphere to prevent oxidation.

2.3. Characterization methods

2.3.1. Surface analysis tests

The surface parameters of the prepared carbon samples were measured by Quantachrome NOVA 2200e series Surface Analyzer. The determination was based on the measurements of the adsorption isotherms of nitrogen at 77 K. All samples were outgassed for 4 h at 200 °C. The surface area was estimated from the BET equation in the relative pressure range of between 0.05 and 0.25, over five adsorption points. The micropore volume was calculated from the Dubinin–Radushkevich (DR) equation. Corresponding mesopore volume was determined by subtracting the micropore volume from the volume of liquid nitrogen adsorbed at relative pressure of 0.95. Pore size distributions were determined using non-local density functional theory for slit-like pore geometry.

2.3.2. XRD measurements

Powder X-ray diffraction (XRD) measurements of the carbonized samples were done with a Bruker AXS advance

powder diffractometer fitted with a Siemens X-ray gun and equipped with Bruker AXS Diffrac PLUS software, using Cu K α radiation ($\lambda = 1.5418 \text{ \AA}$). The sample was rotated (15 rpm) and swept from $2\theta = 5^\circ$ through to 80° using default parameters of the program. The X-ray generator was set to 40 kV at 40 mA. All the XRD measurements were repeated at least three times and the results reported were the average of these measurements.

The XRD patterns were analyzed for the structural parameters using the classical Debye–Scherer equations:

$$L_c = 0.90\lambda/\beta_{002} \cos \theta_{002},$$

$$L_a = 1.94\lambda/\beta_{100/101} \cos \theta_{100/101},$$

$$n = L_c/d_{002},$$

where β is the full width half maxima, FWHM (in radians of theta); n is the number of graphene sheets.

The position of the (002) peak was measured and Bragg's Law was used to calculate the interlayer spacing d_{002} . L_c , L_a and d_{002} values of the carbon microstructures evolved during the pyrolysis of a Turkish lignite were indicated in a recent study [21]. The full widths of (002) and (100)/(101) peaks were calculated at the half maxima (FWHM) with the Bruker AXS Diffrac PLUS software provided with the Bruker AXS advance powder diffractometer of the peak positions of (002) and (100)/(101) peaks.

2.3.3. NMR measurements

Samples were investigated further by ^{13}C CPMAS NMR using an Inova 500 MHz NMR Varian system fitted with a Jacobsen brand CP-MAS probe. ^{13}C CPMAS spectra were acquired at 125.654 MHz using Si_3N_4 rotors set to 6 Hz. Pulses were separated by a 1 s delay. Cross polarization contact time (1 ms), 10 ms data acquisition time, 32 kHz 1 H decoupling field and a spinning rate of 10 kHz were the parameters used during experiments. Two thousand scans were acquired for measurements.

2.3.4. Scanning electron microscopy (SEM)

Samples were examined using a Gemini scanning electron microscope equipped with Leo 32 Supra 35VP field emission scanning system and electron dispersive spectrometer was used for images and analysis, respectively. Imaging was generally done at 2–5 keV accelerating voltage, using the secondary electron imaging technique.

2.3.5. FTIR spectrometry

FTIR spectra of porous carbon samples were measured with a Bruker EQUINOX 55 FTIR spectrometer. Porous carbon samples were dried under a nitrogen atmosphere to prevent oxidation at 110 °C for 24 h. KBr pellets were prepared by grinding 2.5 mg of dry sample with 200 mg of dried KBr. Spectra were obtained with 200 scans at a resolution 2 cm^{-1} .

3. Results and discussion

3.1. SEM, EDS and BET measurements of the mesoporous carbons

Polyfurfuryl alcohol (PFA), a common typical thermosetting resin that forms carbon with a high yield on carbonization [22–24] was used in the present work as carbon precursor for the production of templated carbons. Carbonization experiments were performed with PFA to produce non-templated carbon material at 700 °C. The SEM image of the non-templated carbon materials was presented in Fig. 2. As it can be observed in Fig. 2, this material did not have any structural similarities with the templated carbons (Fig. 3).

The EDS analysis of this material indicated that the carbon content was ca. 100% and the BET analysis revealed that the surface area was 18 m²/g. It is quite interesting that the material was almost completely carbon after the carbonization experiments and the surface area was very low when compared with those of the carbons produced after templation experiments.

FA that was forced to polymerize inside the channels of the natural zeolite was carbonized at different temperatures. The carbon material formed was liberated from the silicate template after HF washing. The BET surface areas of natural zeolite-templated carbons, produced at 700, 800, 900 and 1000 °C, were 397, 350, 405 and 367 m²/g, respectively. It seemed that BET surface areas were not changed greatly with increasing the carbonization temperature.

SEM images of the carbon materials obtained between 700 and 1000 °C are given in Fig. 3. The morphological similarity between the template and their carbon replicas was obvious from SEM images (Fig. 1). At the micrometer level, the carbon material templated with the natural zeolite contained the same morphology as the zeolite. The natural

zeolite template which contained mainly micro and mesopores (Table 1), demonstrated some heterogeneous characteristics: mainly groups of granular-type crystals, interrelated by a web-like structure. Both of these characteristics could be found in the templated carbons. The SEM images of the carbons produced after templating and carbonizing at different temperatures gave the impression that the zeolite framework was retained in the templated porous carbon.

Fig. 4 shows the N₂ adsorption–desorption isotherms of the carbon materials produced. Nitrogen adsorption isotherms of the zeolite-templated carbon samples can be classified as type-IV isotherm. The relatively sharp increase in volume adsorbed at about $P/P_0 = 0.8$ is an indication of the presence of mesopores [25] which was confirmed by the pore size distributions curves shown in Fig. 5. Pore size distribution of the carbons are presented in Fig. 5. In all the samples the pore size distribution was very similar indicating formation of comparable pore structure in the carbons produced. Average pore diameter of the porous carbons, produced in the range of 700–1000 °C, was ca. 5–10 nm indicating presence of a mesoporous framework in the carbons produced in the present work, which corresponded to mesopores according to the classification of IUPAC [3]. Therefore, carbon materials made in the present work using the natural zeolite as templates contained mainly mesopores.

Results of the EDS analyses of natural zeolite-templated carbons prepared at different temperatures are presented in Table 2. The porous carbon samples obtained at 700 °C, 800 °C, 900 °C and 1000 °C contained 91.1%, 95.8%, 98.8% and 99.0% C, respectively. Atomic O/C ratio decreased from 0.026 to 0.001 as the carbonization temperature was increased from 700 °C to 1000 °C. Carbonization at higher temperatures increased the carbon content and decreased the oxygen content in the product. The success of the demineralization step was indicated by both the high

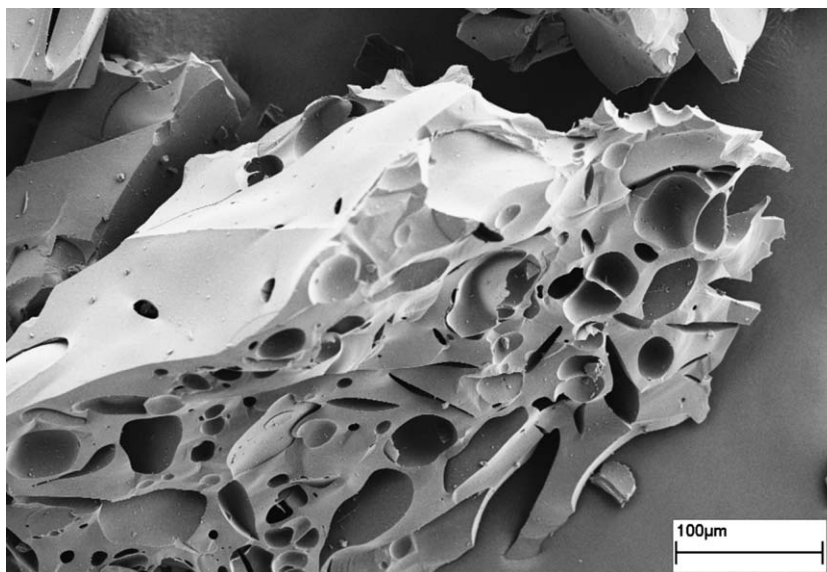


Fig. 2. SEM image of non-templated polymerized and carbonized furfuryl alcohol.

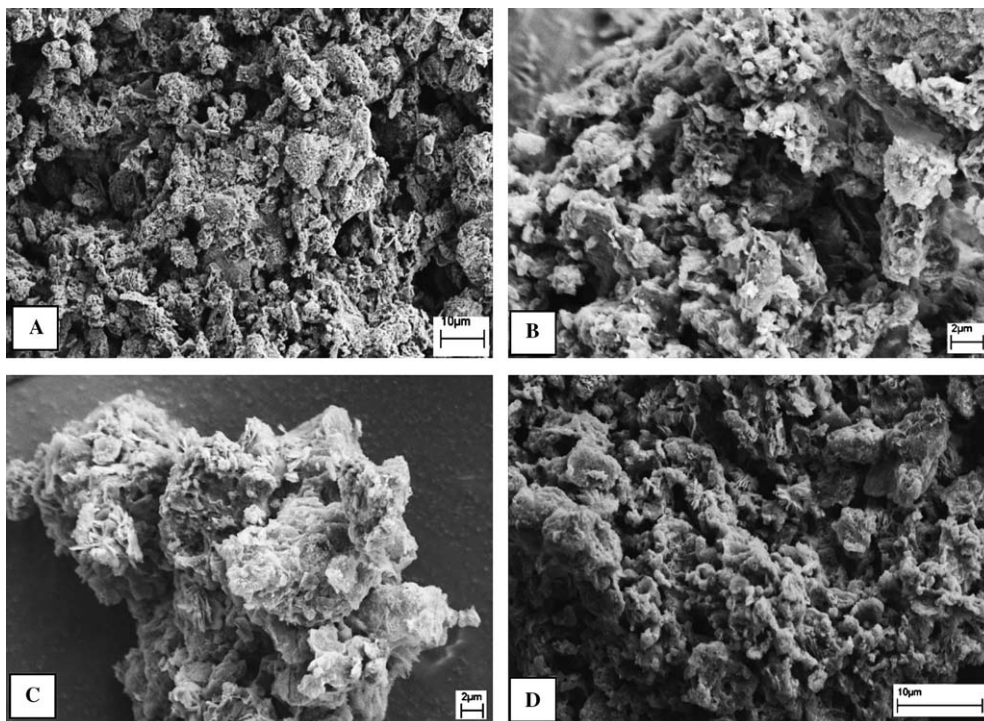


Fig. 3. SEM images of natural zeolite-templated carbon, produced at (A) 700 °C, (B) 800 °C, (C) 900 °C and (D) 1000 °C.

carbon content (typically above 90 wt.%) and the small quantities of silicon and aluminium present (usually less than 1%). Low quantities of Mg in the samples might be due to the presence of magnesium carbides, MgC_2 and Mg_2C_3 , that were produced in the temperature range of 500–700 °C [26].

The natural zeolite acted as a catalyst besides being used as the template in the sol–gel process where TEOS together with FA was employed. Hydroxyl groups adjacent to aluminium in the aluminosilicate framework catalyze the polymerization reaction of the FA as Brønsted acid sites [27]. After dissolution of silica network with HF, the obtained material contained ca. 95% elemental carbon and the BET surface area of this material was measured as 804 m²/g. The surface area of the material produced was much higher than that of the carbon material produced without templation. The effect of zeolite templation in the production of high-surface material was very obvious after these experiments.

The BET surface area of the carbon material produced from the carbonization of FA within the channels of the natural zeolite at 700 °C was measured as 397.2 m²/g, whereas addition of 10% TEOS that was also used as template increased the BET surface area to 430.0 m²/g. The BET surface area of the porous carbons obtained by template carbonization within taeniolite framework was reported previously to be 400 m²/g [28]. Porous carbon materials synthesized using different precursors [29] inside channels of the Y, β , and ZSM-5 zeolites had BET surface areas that changed between 458 and 504 m²/g for acrylonitrile, between 245 and 636 m²/g for pyrene as carbon sources.

3.2. ¹³C NMR and FTIR spectra

All of the ¹³C NMR spectra of the carbons produced at different carbonization temperatures contained peaks due to similar chemical functionalities with slight variations in the intensities. Therefore, the ¹³C NMR spectrum of natural zeolite-templated carbon that was produced at 700 °C was chosen to represent the characteristics of all of the ¹³C NMR spectra (Fig. 6). All of the peaks in the ¹³C NMR spectra were significant peaks and there were no side bands whatsoever. The observed peaks were assigned to the following functionalities: the peaks near 30 ppm, 80 ppm and 127 ppm might be due to sp³-hybridized carbon [29], sp-hybridized carbon at and sp²-hybridized carbon in graphite or graphite-like domains [30–33], respectively. The peak near 175 ppm might be due to alkoxy and OH substituted carbon. The temperature 700 °C is considered as medium range temperature in the carbonization most of the carbon precursors and the presence of all types of carbon bands at this range of temperatures seemed to be quite obvious. The peak at 40 ppm could be attributed to the presence of –CH and –CH₂ groups and the signal at 39 ppm might be as a result of crosslinking between oligo FA and PFA sequences [34] and due to the crosslinking through these methylene groups [35]. The ¹³C signals for the olefinic carbon atoms were not resolved, but they were clearly detectable in the solid-state ¹³C NMR spectrum as a broad signal between 120 and 140 ppm [34].

FTIR spectra of porous carbons obtained at different carbonization temperatures are presented in Fig. 7. In all of the recorded spectra, a band due to O–H stretching

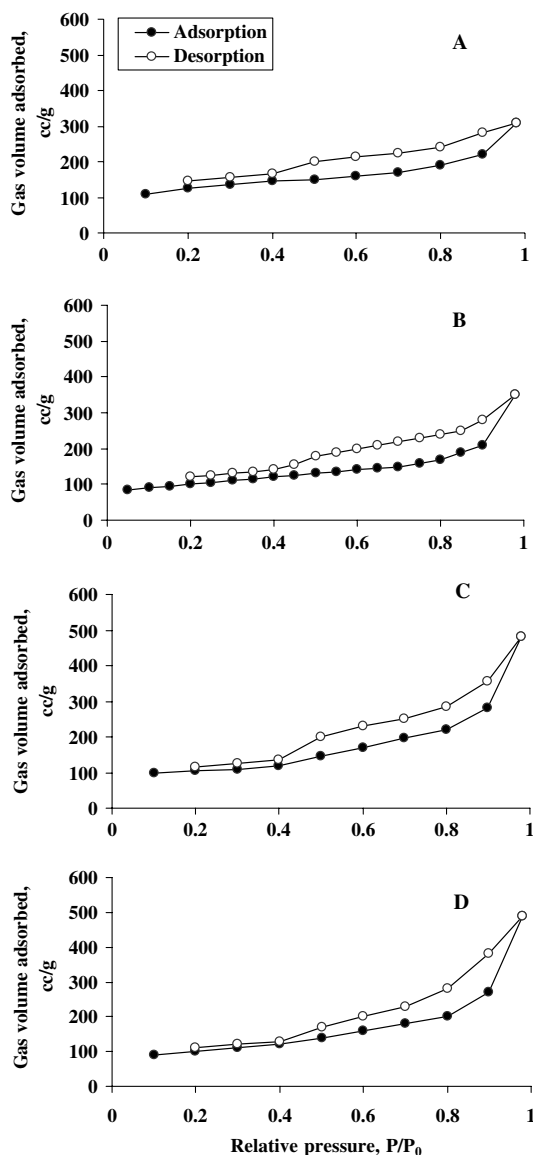


Fig. 4. N_2 adsorption/desorption isotherms of natural zeolite-templated carbons, produced at (A) 700 °C, (B) 800 °C, (C) 900 °C and (D) 1000 °C.

vibrations in the 3500–3400 cm^{-1} range that indicated existence of hydroxylic groups was observed. The asymmetry of this band at lower wavenumbers indicates the presence of the strong hydrogen bonds in the products [36–38]. Peaks observed at 3135 cm^{-1} , between 1450–1200 cm^{-1} and 1259 cm^{-1} were as the result of =C–H stretching band, –C=C–H in-plane C–H bend and –C≡C–H bend overtone vibrations, respectively [37,38].

The presence of bands of –CH₃ or –CH₂– structures in the ranges of 2946–2958 cm^{-1} , 2915–2916 cm^{-1} and 2847–2854 cm^{-1} in all of the spectra suggested the existence of some asymmetric and symmetric C–H stretching vibrations, sp^3 hybridized carbons, in the porous carbons [38]. The intensities of these bands decreased with increasing carbonization temperature.

The band in the region of 1631–1664 cm^{-1} was probably due to C=C stretching band present in the carbons and the

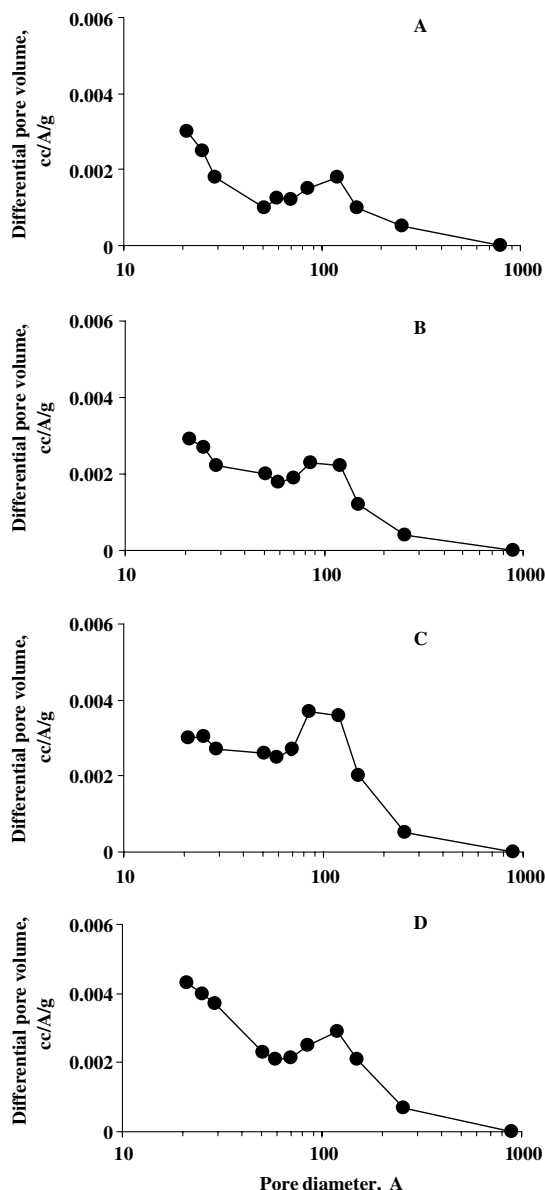


Fig. 5. Pore size distribution of natural zeolite-templated carbons, produced at (A) 700 °C, (B) 800 °C, (C) 900 °C and (D) 1000 °C.

Table 2
EDS analyses of natural zeolite templated carbons

Element	Atomic C [at.%]			
	700 °C	800 °C	900 °C	1000 °C
Carbon	91.1	95.8	98.8	99.0
Fluorine	5.4	2.2	0.8	0.7
Magnesium	0.1	0.1	0	0
Aluminium	0.1	0.3	0.1	0.1
Oxygen	3.2	1.5	0.3	0.2
Silicon	0	0.1	0	0
O/C	0.026	0.012	0.002	0.001

absorption maximum of this band shifted towards lower wavenumbers with increasing carbonization temperature until 1000 °C. The reason for this shift might be because of the conjugation of C=C bond with another C=C bond,

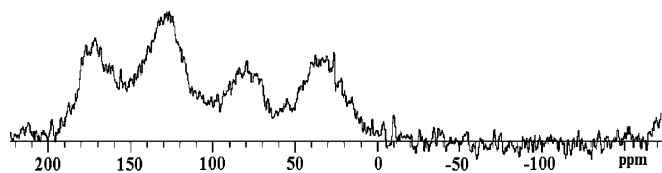


Fig. 6. ^{13}C NMR spectrum of natural zeolite-templated carbon, produced at 700 °C.

an aromatic nucleus, or a C–O bond [39]. The band around 1735 cm^{-1} was attributed to AlH_4^+ due to undissolved zeolite residues and to carboxylic groups [37]. Broad bands at $1300\text{--}1000\text{ cm}^{-1}$ have been assigned to C–O stretching [40].

Mononuclear and polynuclear aromatic hydrocarbons generally give four bands in the following regions, $1635\text{--}1600\text{ cm}^{-1}$, $1595\text{--}1570\text{ cm}^{-1}$, $1520\text{--}1460\text{ cm}^{-1}$ and $1470\text{--}1415\text{ cm}^{-1}$ [37] but not all four bands appear in each case. The FTIR spectra measured in the present study contained peaks that fell in to these regions. This could be an indication that carbons produced contained some aromatic patterns in their structures.

The general conclusion obtained from ^{13}C NMR and FTIR spectra was that the carbons produced in the carbonization range of $700\text{--}1000\text{ °C}$ still contained certain oxygen and hydrogen functional groups and aromatic structures. The products obtained were not absolutely pure carbons obtained at medium carbonization temperatures but as the temperature of the carbonization was increased to 1000 °C , the percentage of the elemental carbon in the products seemed to increase to values close to 100.

3.3. X-ray diffraction patterns

The powder XRD pattern of the zeolite template (Fig. 8) is characterized by many peaks due to its structure ordering. Some of these peaks were still observable in the powder XRD pattern of the mesoporous carbons: at $2\theta = 7.5^\circ$, 30° and 32° (Fig. 9), demonstrating that the framework of the zeolite survived the high temperature treatment up to 1000 °C .

The interlayer spacing (d_{002}) of the carbon is traditionally used to estimate the graphitization degree of carbons and, in general, growing disorder in the materials is reflected in increased values of d_{002} . The d_{002} values of the crystal structures in the carbons of the present work were calculated from the XRD patterns of the carbons at different carbonization temperatures (Fig. 9). The vanishing of the zeolite peaks with the exception of the (101) at $2\theta = 8^\circ$ and the appearance of a broad (002) peak at around $2\theta = 26^\circ$ and a low intensity (100) peak at around $2\theta = 40^\circ$ approve that the template elimination process was correctly done. The (101) peak was undoubtedly kept even after the removal of the template. The presence of this peak implied that the structural regularity of the zeolite was preserved over extended distances in the carbons [18].

The resultant porous carbons exhibited two large diffraction peaks near $2\theta = 26^\circ$ and $2\theta = 40^\circ$, which were charac-

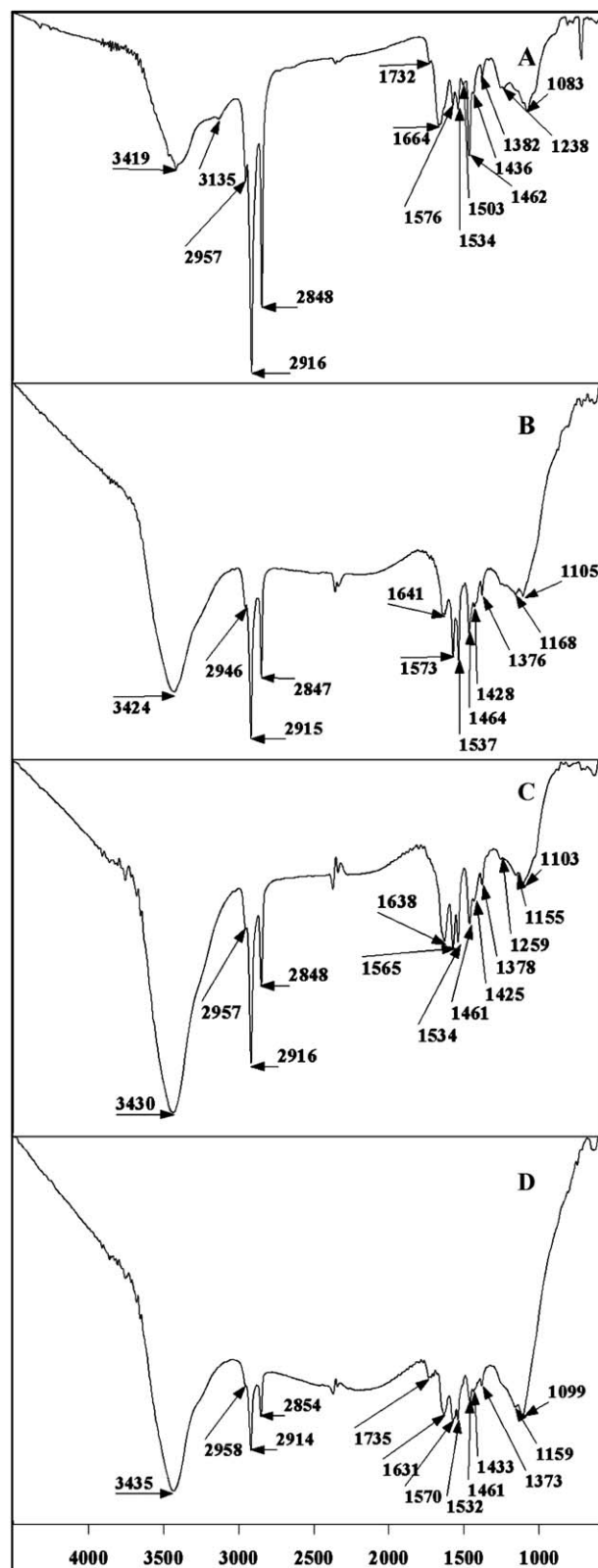


Fig. 7. FT-IR spectra of natural zeolite-templated carbons, produced at (A) 700 °C, (B) 800 °C, (C) 900 °C and (D) 1000 °C.

teristic of a disordered carbonaceous structure. By analogy with disordered carbon structures, the two peaks could be indexed as the (002) and (100) reflections of the hexagonal

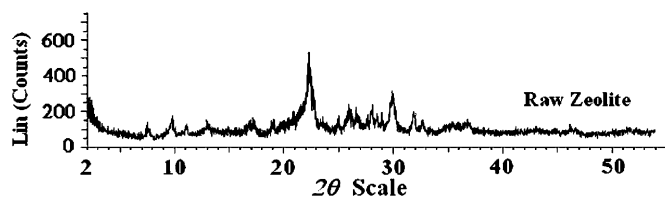


Fig. 8. Powder X-ray diffractogram of Turkish Manisa Gördes natural zeolite.

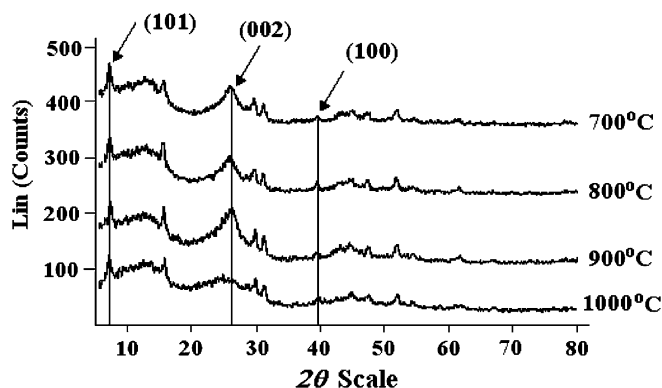


Fig. 9. Powder X-ray diffractograms of natural zeolite-templated porous carbons produced at different carbonization temperatures.

structure of graphite. A broad peak at $2\theta = 26^\circ$ represented (002) reflection of carbon due to the stacking structure of aromatic layers [21].

The d_{002} values of the carbon materials synthesized by carbonization of PFA in the channels of zeolite are presented in Table 3. The results put forward in the present work might be considered as indications to the presence of turbostratic (fully disordered) structures in the carbons obtained in the temperature range of 700–1000 °C. The decrease in the intensity of the (002) peaks over the same temperature range could be explained by the loss of amounts of carbon from large turbostratic crystallites. This was in accordance with the expectation that carbon losses would be observed as the temperature was increased during the carbonization reactions [21]. Crystallite growth involves mass transport processes and may be due to either motion and mergence of layers coming in contact or atomic diffusion [21].

Addition of 10% TEOS into the system caused the d_{002} value to decrease from 0.36 nm to 0.35 nm, at 700 °C. The relative intensities of (002) peaks were 1.0, 0.9, 0.7 and 0.7 for 700 °C, 800 °C, 900 °C and 1000 °C, respec-

tively. The d_{002} intensities decreased with increasing temperature after 700 °C. The decrease of the intensity of the (002) peaks in the present work could be explained by the loss of carbon structures during carbonization at higher temperatures. Barata-Rodrigues et al. [18] observed a value 0.342 nm for d_{002} , for the zeolite-templated carbon. This value was considered to be larger than that of the ideal graphite (0.3354 nm), thus this could be taken as an indication to the carbon produced contained some disordered structures. The d_{002} value of TEOS–FA carbon material produced in the present work was 0.36 nm and therefore this value was indicating that the carbon was formed with some degree of disorder. Sakintuna et al. [21] recently reported d_{002} values of activated carbons in the range of 0.35–0.39 nm.

It was previously reported that [30] the XRD traces of the templated carbons contained a sharp peak around $2\theta = 6^\circ$, indicating that these carbons presented a structural regularity. In addition to this peak, absence of the broad peak near $2\theta = 26^\circ$ indicated also to the absence of stacking of carbon layers. Graphene layers are the basic building block of carbon particles and these layers exhibit numerous distortions and discontinuities. Some regions, however, have a more regular, graphite-like arrangement. The dimensions of these graphitic domains are characterized by the average stacking height of the parallel layers in the “*c*” direction (L_c) and by the average diameter of the “*c*” parallel layers in the “*a*” direction (L_a). These two dimensions can be determined by Debye–Sherrer equation. The L_c and L_a values of non-templated carbons were 2 nm and 6 nm, respectively and those of TEOS–FA carbons were 2 nm and 5 nm, respectively.

L_c values of the carbons increased from 3 nm to 7 nm, and average number of graphene sheets increased from 8 to 19 when the carbonization temperature was increased from 700 °C to 1000 °C (Table 3). The L_c value of the carbon produced after the addition of 10% TEOS and carbonization at 700 °C, was measured as 3 nm. Similar results were reported recently by Sakintuna et al. [21]. Kercher and Nagle [41] reported that while increasing carbonization temperature, the crystallite boundary area was observed to decrease and turbostratic crystallite growth and number of graphene sheets seemed to increase. The reason for the increase in the stacking height was related to heat treatment temperature only. Previously three temperatures were found to be critical in the carbonization of PFA [42]. The molecular structure of PFA is degraded at about 400 °C at which carbonization begins, and when the temperature

Table 3
Change of structural characteristics of carbons at different temperatures

Carbonization temperature (°C)	Stacking height, L_c (nm)	Interlayer spacing, d_{002} (nm)	Average number of graphene sheets, n	Full width half maxima, FWHM (radians of θ)	Relative intensity of (002) peak
700	3	0.36	8	2.9	1.0
800	5	0.35	14	1.6	0.9
900	6	0.35	18	1.3	0.7
1000	7	0.35	19	1.2	0.7

reaches 550 °C a large number of small graphitic crystalline nuclei are formed. As the temperature is further increased to about 700 °C nuclei growth and large crystalline grains are observed. The size of the microcrystallites increased quickly with increasing the carbonization temperature. The growth of the carbon layer plane might be due to the increase of van der Waals forces between the layers, which resulted in increases of the stacking number. Hence the coalescence of the units was probably accelerated in the temperatures between 700 °C and 1000 °C, as it was also observed in the present work.

4. Conclusions

The porous carbon samples obtained between 700 °C and 1000 °C contained 91.1–99.0% elemental carbon. Atomic O/C ratio decreased from 0.026 to 0.0015 at the same temperature range.

The SEM images of the carbons showed that they had similar macroscopic appearances with the native zeolite. The surface area of the carbons produced within the template was in the range of 400–800 m²/g while the surface area of the carbon produced without templation was only 18 m²/g. Templation seemed to increase the surface area of the porous carbons produced. The average pore diameter distribution of the templated carbons was measured as ca. 5–10 nm for all the carbons produced in the range of 700–1000 °C; this was the indication to the presence a mesoporous framework within the carbons produced in the present work.

The ¹³C NMR and FTIR spectra revealed that the carbons produced in the carbonization range of 700–1000 °C still contained some hydrogen and oxygen containing functional groups. The XRD results put forward indications to the presence of turbostratic structures and preservation of the structural regularity of the zeolite over extended distances in the carbons.

Acknowledgments

The authors extend their gratitude to Professor Zeki Aktaş of Department of Chemical Engineering of Ankara University, who kindly performed the BET analyses of the carbons produced in the present work.

References

- [1] B. Sakintuna, Y. Yürüm, *Ind. Eng. Chem. Res.* 44 (2005) 2893.
- [2] J.E. Hampsey, Q. Hu, Z. Wu, L. Rice, J. Pang, Y. Lu, *Carbon* 43 (2005) 2977.
- [3] R. Ryoo, S.H. Joo, M. Kruk, M. Jaroniec, *Adv. Mat.* 13 (2001) 677.
- [4] S. Fan, M.G. Chapline, N.R. Franklin, T.W. Tomblor, A.M. Cassell, H. Dai, *Science* 283 (1999) 512.
- [5] S. Subramoney, *Adv. Mater.* 10 (1998) 1157.
- [6] IUPAC Compendium of Chemical Terminology, second ed., vol. 46, 1997, p. 1976.
- [7] R.V. Parthasarathy, C. Martin, *Nature* 369 (1994) 298.
- [8] S.A. Johnson, P.J. Ollivier, T.E. Mallouk, *Science* 282 (1999) 963.
- [9] C.R. Martin, *Adv. Mater.* 3 (1991) 457.
- [10] J.D. Klein, R.D.I. Herrick, D. Palmer, M.J. Sailor, C.J. Brumlik, C.R. Martin, *Chem. Mater.* 5 (1993) 902.
- [11] C.R. Martin, *Chem. Mater.* 8 (1996) 1739.
- [12] A.J.G. Zarbin, M.-A. De Paoli, O.L. Alves, *Synth. Met.* 99 (1999) 227.
- [13] T. Kyotani, T. Nagai, S. Inoue, A. Tomita, *Chem. Mater.* 9 (1997) 609.
- [14] J. Rodriguez-Mirasol, T. Cordero, L.R. Radovic, J.J. Rodriguez, *Chem. Mater.* 10 (1998) 550.
- [15] S.A. Johnson, E.S. Brigham, P.J. Ollivier, T.E. Mallouk, *Chem. Mater.* 9 (1997) 2448.
- [16] Z. Ma, T. Kyotani, A. Tomita, *Carbon* 40 (2002) 2367.
- [17] T. Kyotani, Z. Ma, A. Tomita, *Carbon* 41 (2003) 1451.
- [18] P.M. Barata-Rodrigues, T.J. Mays, G.D. Moggridge, *Carbon* 41 (2003) 2231.
- [19] K. Matsuoka, Y. Yamagishi, T. Yamazaki, N. Setoyama, A. Tomita, T. Kyotani, *Carbon* 43 (2005) 876.
- [20] A. Garsuch, O. Klepel, *Carbon* 43 (2005) 2330.
- [21] B. Sakintuna, Y. Yürüm, S. Çetinkaya, *Energy Fuels* 18 (2004) 883.
- [22] A. Shindo, K. Izumino, *Carbon* 32 (1994) 1233.
- [23] X. Zhang, D.H. Solomon, *Chem. Mater.* 11 (1999) 384.
- [24] M. Domingo-Garcia, F.J. Lopez-Garzon, M. Perez-Mendoza, *Carbon* 38 (2000) 555.
- [25] A.S. Maria Chong, X.S. Zhao, A.T. Kustedjo, S.Z. Qiao, *Micropor. Mesopor. Mater.* 72 (2004) 33.
- [26] F.A. Cotton, G. Wilkinson, *Advanced Inorganic Chemistry*, third ed., Wiley, New York, 1972.
- [27] H. Darmstadt, C. Roy, S. Kaliaguine, T.-W. Kim, R. Ryoo, *Chem. Mater.* 15 (2003) 3300.
- [28] T.J. Bandosz, J. Jagie, K. Putyera, J.A. Schwarz, *Chem. Mater.* 8 (1996) 2023.
- [29] C.J. Meyers, S.D. Shah, S.C. Patel, R.M. Sneeringer, C.A. Bessel, N.R. Dollahon, R.A. Leising, E.S. Takeuchi, *J. Phys. Chem. B* 105 (2001) 2143.
- [30] C.G. Bac, P. Bernier, S. Latil, V. Jourdain, A. Rubio, S.H. Jhnag, S.W. Lee, Y.W. Park, M. Hozinger, A. Hirsch, *Curr. Appl. Phys.* 1 (2001) 149.
- [31] Z. Ma, T. Kyotani, Z. Liu, O. Terasaki, A. Tomita, *Chem. Mater.* 13 (2001) 4413.
- [32] H. Darmstadt, C. Roy, S. Kaliaguine, G. Xu, M. Auger, A. Tuel, *Carbon* 38 (2000) 1279.
- [33] M.M. Golzan, P.B. Lukins, D.R. Mackenzie, A.M. Vassalo, J.V. Hanna, *Chem. Phys.* 193 (1995) 167.
- [34] H. Müller, P. Rehak, C. Jager, J. Hartmann, N. Meyer, S. Spange, *Adv. Mater.* 12 (2000) 1671.
- [35] A.J.G. Zarbin, R. Bertholdo, M.A.F.C. Oliveira, *Carbon* 40 (2002) 2413.
- [36] S. Biniak, G. Szymanski, J. Siedlewski, A. Swietkowski, *Carbon* 35 (1997) 1799.
- [37] G. Svehla, *Comprehensive Analytical Chemistry*, New York, 1976.
- [38] Y. Yürüm, N. Altuntas, *Fuel Sci. Technol. Int.* 12 (1994) 1115.
- [39] M.-W. Jung, K.-H. Ahn, Y. Lee, K.-P. Kim, J.-S. Rhee, J.T. Park, K.-J. Paeng, *Microchem. J.* 70 (2001) 123.
- [40] J. Guo, A.C. Lua, *Separat. Purif. Technol.* 18 (2000) 47.
- [41] A. Kercher, D.C. Nagle, *Carbon* 41 (2003) 15.
- [42] Z. Wang, Z. Lu, X. Huang, R. Xue, L. Chen, *Carbon* 36 (1998) 51.